Analysis of Global Systems, Support Centers, and Weather Units Aviation

Gabriela-Liliana STROE[1,2], Mihaela-Luminita COSTEA*,[1,2]

*Corresponding author
[1]Faculty of Aerospace Engineering, University POLITEHNICA of Bucharest,
Splaiul Independentei 313, 060042, Bucharest, Romania
[2]INCAS – National Institute for Aerospace Research "Elie Carafoli",
B-dul Iuliu Maniu 220, Bucharest 061126, Romania,
ing.stroe@yahoo.com, costea.mihaela@incas.ro*

DOI: 10.13111/2066-8201.2023.15.3.8

Received: 08 June 2023/ Accepted: 02 August 2023/ Published: September 2023

Abstract: *This paper examines the analysis of meteorological observations concerning wind direction and intensity. These observations are typically found in regular weather reports, which play a crucial role in the safe arrival and departure of aircraft, and provide vital information about current conditions along airport runways. To ensure accuracy, the locations of wind sensors along runways must be specified in routine weather reports. Furthermore, reported wind information data should be linked to the specific sections of the runway for which the data are representative. In cases where wind observations are available from multiple tracks, the relevant track information should also be included in routine weather reports, alongside the corresponding wind data. For surface wind conditions, the observations included in the METAR reports should accurately represent the entire runway, and it is important to indicate the specific runway or runway sections to which the observations pertain.*

Key Words: *wind direction, routine weather report, numerical simulation*

1. INTRODUCTION

The global atmospheric circulation is primarily driven by the differential radiative heating caused by solar radiation absorption at the Earth's surface. This process significantly impacts the flight of aircraft. In low latitudes, solar radiation absorption exceeds long-wavelength radiation emission into space, whereas in high latitudes, particularly during winter in the respective hemisphere, the emission of long-wave radiation dominates over solar radiation absorption. The combined atmospheric and oceanic general circulation worldwide facilitates the transfer of heat meridionally (along latitudes) and vertically, allowing for the attainment of thermal equilibrium. Solar radiation heating primarily takes place within the atmosphere through the release of latent heat during convective processes occurring in clouds. The zonal average patterns of key radiative elements like carbon dioxide, ozone, and cloud cover are considered in these processes. Mathematical models for general circulation commonly employ global aerodynamic formulas to parameterize the momentum, heat, and moisture fluxes within the boundary layer. This allows for a representation of the interactions between the atmosphere and the Earth's surface in the models. In atmospheric modeling, the flow dynamics are typically influenced by the combination of horizontal velocity magnitude in the lower atmosphere and

the disparity between boundary conditions and the corresponding variable values in the lowest atmosphere. This relationship allows for the estimation of fluxes and transports within the model. The water cycle, encompassing the movement and distribution of water in the atmosphere, is described using a combination of parameterization and explicit prediction. This approach considers various processes such as evaporation, condensation, and precipitation, taking into account the physical and thermodynamic properties of water vapor, where the measurement of absolute humidity is the weight of water vapor in the unit volume of air. [1] To maintain radiative balance in the model, the predicted moisture distribution is utilized. This information is then used to determine the arrangement of cloud layers and the occurrence of large-scale precipitation. When the predicted moisture levels exceed 100%, vapor condensation occurs to reduce the mixing ratio to a saturation point or even lower. This ensures that the condensed vapor is sufficient to maintain a state of saturation and prevent excessive moisture levels in the atmosphere. This process is crucial for determining the distribution of clouds and the occurrence of precipitation within the modeled system. Furthermore, to represent the distribution of convective clouds and associated precipitation, parameterizations based on the average thermal state and the structure of the moisture field are employed. These parameterizations consider the statistical characteristics of convective processes and the spatial distribution of moisture to simulate the occurrence and distribution of convective clouds and precipitation within the model.

2. STATE OF ART FOR WEATHER UNITS AVIATION

The Lorentz Cycle of Energy (LCE) can be succinctly described by incorporating the average zonal energy, turbulent kinetic energy, and available potential energy, as outlined in the mathematical algorithm developed in the referenced paper.

In a dry atmosphere where turbulent diabatic processes are primarily restricted to radiation and diffusion, the diabatic generation of available turbulent potential energy should be negative. This is because thermal radiation emitted into the atmospheric space increases with rising temperatures, which in turn reduces the horizontal thermal contrast within the atmosphere.

However, in the Earth's atmosphere, the presence of clouds and precipitation significantly modifies the distribution of turbulent diabatic processes (represented by R'). These atmospheric phenomena have a substantial impact on the distribution and generation of available turbulent potential energy within the Lorentz Cycle of Energy. The influence of clouds and precipitation alters the thermal contrast and introduces additional factors that affect the dynamics of the energy cycle [2].

Current estimates show that EN - R' is positive and equal to almost half of the value of R barred. The observed atmospheric energy cycle, as given by the Eulerian averaging formalism, is comparable to the observation that unsteady baroclinic eddies are the main perturbations responsible for the midlatitude energy exchange. The loss of kinetic energy through turbulent stresses is replaced by turbulent motions, and the main ones responsible for transporting heat to the pole, to counterbalance the radiation deficit in polar regions, atmospheric eddies, play a significant role. Besides transient baroclinic eddies, stationary orographic waves and free Rossby waves can also contribute significantly to the transport of heat toward the poles, helping to balance the radiation deficit in the polar regions. In the mid-latitudes, the conversion of mean available potential energy to mean kinetic energy through circulation in symmetric cells tends to show a small and negative behavior. This implies that the energy tends to dissipate rather than contribute to the overall circulation in those regions. However, in the tropics, this conversion process has a positive impact and plays a significant role in sustaining the mean

Hadley circulation, which is responsible for the large-scale tropical atmospheric circulation patterns. Many mathematical models that study the global general circulation employ primitive equations expressed in sigma coordinates. This choice allows for the retention of the benefits associated with isobaric coordinates while simplifying the definition of surface boundary conditions. The Lorenz energy cycle encompasses the zonal-mean, eddy kinetic and available potential energies, representing large-scale, small-scale, and potential energy in the atmosphere, respectively:

$$\bar{K} \equiv \left\langle \rho_0 \frac{\bar{u}^2}{2} \right\rangle \tag{1}$$

$$K' \equiv \left\langle \rho_0 \frac{\overline{u'^2} + \overline{v'^2}}{2} \right\rangle \tag{2}$$

$$\bar{P} \equiv \frac{1}{2} \left\langle \frac{\rho_0}{N^2} \left(\frac{\partial \bar{\Phi}}{\partial z} \right)^2 \right\rangle \tag{3}$$

$$P' \equiv \frac{1}{2} \left\langle \frac{\rho_0}{N^2} \overline{\left(\frac{\partial \Phi'}{\partial z} \right)^2} \right\rangle \tag{4}$$

The energy transformations [2]:

$$[\bar{P} \cdot \bar{K}] \equiv \left\langle \rho_0 \bar{w} \frac{\partial \bar{\Phi}}{\partial z} \right\rangle \tag{5}$$

$$[P' \cdot K'] \equiv \left\langle \rho_0 \overline{w'} \frac{\partial \Phi'}{\partial z} \right\rangle \tag{6}$$

$$[K' \cdot \bar{K}] \equiv \left\langle \rho_0 \overline{u'v'} \frac{\partial \bar{u}}{\partial y} \right\rangle \tag{7}$$

$$[P' \cdot \bar{P}] \equiv \left\langle \frac{\rho_0}{N^2} v' \overline{\frac{\partial \Phi'}{\partial z}} \frac{\partial^2 \bar{\Phi}}{\partial y \, \partial z} \right\rangle \tag{8}$$

And the source and sinks [2]:

$$\bar{R} \equiv \left\langle \frac{\rho_0}{N^2} \frac{\kappa \bar{J}}{H} \frac{\partial \bar{\Phi}}{\partial z} \right\rangle \tag{9}$$

$$R' \equiv \left\langle \frac{\rho_0}{N^2} \overline{\frac{\kappa J'}{H}} \overline{\frac{\partial \Phi'}{\partial z}} \right\rangle \tag{10}$$

$$\bar{\varepsilon} \equiv \langle \rho_0 \bar{u} \bar{X} \rangle \tag{11}$$

$$\varepsilon' \equiv \langle \rho_0 (\overline{u'X'} + \overline{v'Y'}) \rangle \tag{12}$$

Integrating over the entire volume [2]:

$$\frac{d}{dt}\langle\frac{\rho_0\bar{u}^2}{2}\rangle = +\langle\rho_o\bar{\Phi}\frac{\partial\bar{v}}{\partial \mathrm{y}}\rangle + \langle\rho_o\overline{u'v'}\rangle + \langle\rho_0\bar{u}\bar{X}\rangle \tag{13}$$

$$\frac{d}{dt}\langle\frac{\rho_0}{2N^2}\left(\frac{\partial\bar{\Phi}}{\partial \mathrm{z}}\right)^2\rangle = -\langle\rho_0\bar{w}\frac{\partial\bar{\Phi}}{\partial \mathrm{z}}\rangle + \langle\frac{\rho_0 k\bar{J}}{N^2H}\left(\frac{\partial\bar{\Phi}}{\partial \mathrm{Z}}\right)\rangle - \langle\frac{\rho_0}{N^2}\frac{\partial\bar{\Phi}}{\partial \mathrm{Z}}\frac{\partial}{\partial \mathrm{Y}}\left(\overline{v'\frac{\partial\Phi'}{\partial \mathrm{z}}}\right)\rangle \tag{14}$$

$$\frac{d}{dt}\langle\rho_0\frac{\overline{u'^2}+\overline{v'^2}}{2}\rangle = +\langle\rho_0\overline{\Phi'\left(\frac{\partial\Phi'}{\partial \mathrm{x}}+\frac{\partial v'}{\partial \mathrm{y}}\right)}\rangle - \langle\rho_0\overline{u'v'}\frac{\partial\bar{u}}{\partial \mathrm{y}}\rangle + \langle\rho_0(\overline{u'X'}+\overline{v'Y'})\rangle \tag{15}$$

$$\frac{d}{dt}\langle\frac{\rho_0}{2N^2}\overline{\left(\frac{\partial\Phi'}{\partial \mathrm{z}}\right)^2}\rangle = -\langle\rho_0 w'\frac{\overline{\partial\Phi'}}{\partial \mathrm{z}}\rangle + \langle\frac{\rho_0 k\overline{J'\,\partial\Phi'}}{N^2H}\rangle - \langle\frac{\rho_0}{N^2}\left(\frac{\partial^2\bar{\Phi}}{\partial \mathrm{z}\,\partial \mathrm{y}}\right)\left(\overline{v'\frac{\partial\Phi'}{\partial \mathrm{z}}}\right)\rangle \tag{16}$$

Equations (3), (13), (14), (15) and (16) can then be expressed in the simple form [2]:

$$\frac{d\bar{K}}{dt} = [\bar{P}\cdot\bar{K}] + [K'\cdot\bar{K}] + \bar{\varepsilon} \tag{17}$$

$$d\bar{P}/dt = -[\bar{P}\cdot\bar{K}] + [P'\cdot\bar{P}] + \bar{R} \tag{18}$$

$$dK'/dt = [P'\cdot K'] - [K'\cdot\bar{K}] + \varepsilon' \tag{19}$$

$$dP'/dt = -[P'\cdot K'] - [P'\cdot\bar{P}] + R' \tag{20}$$

Rate of change of total energy (kinetic plus available potential) [2]:

$$d(\bar{K}+K'+\bar{P}+P')/dt = \bar{R}+R'+\bar{\varepsilon}+\varepsilon' \tag{21}$$

Hence, in order to maintain energy balance within the Lorentz Cycle of Energy, the production of available potential energy through zonal-mean and eddy diabatic processes must be in equilibrium with the dissipation of mean plus eddy kinetic energy [2]. This balance ensures that the energy inputs and outputs within the system are matched, leading to a stable and consistent energy cycle. The zonal-mean and eddy diabatic processes contribute to the production of available potential energy, which represents the potential for work to be done by the atmospheric system. On the other hand, the dissipation of mean plus eddy kinetic energy accounts for the loss of kinetic energy due to various processes such as friction, turbulence, and other forms of energy dissipation. By balancing the dissipation of kinetic energy, the Lorentz Cycle of Energy achieves energy equilibrium through the production of available potential energy. This equilibrium is crucial for maintaining stability and governing the overall behavior of the atmospheric system, such that:

$$\bar{R}+R' = -\bar{\varepsilon}-\varepsilon' \tag{22}$$

Moisture continuity equation, which can be expressed as [2]:

$$\frac{D}{Dt}(q_v) = P_v \tag{23}$$

q_v -water vapor mixing ratio

P_v – the sum of all sources, sinks

$\rho_s(x, y, t)$ – the evolution of the surface pressure

Transformed continuity equation [2]:

$$\frac{\partial \rho_0}{\partial t} + \bar{V} \cdot (\rho_0 V) + \rho_s \frac{\partial \dot{\sigma}}{\partial \sigma} = 0 \tag{24}$$

Integrating (24) vertically and using the boundary condition $\dot{\sigma} = 0$ and $\sigma = 0$, the result [2]:

$$\frac{\partial p_S}{\partial t} = -\int_0^1 \nabla \cdot (p_S V) d\sigma \tag{25}$$

The leading-order Taylor series approximation [2]:

$$T(R_0 + \delta R) = T(R_0) + \frac{\partial T}{\partial R}\Big|_{R_0} \delta R \tag{26}$$

T - temperature

R - parameter

R0 - value for the unperturbed climate

When the radiative heating is perturbed by a certain value, denoted as δR, the system exhibits a linear response. This means that the system's response is directly proportional to the magnitude of the perturbation:

$$\partial T = \frac{\partial T}{\partial R}\Big|_{R_0} \delta R = \lambda \delta R \tag{27}$$

λ - climate sensitivity parameter

Feedback mechanisms can amplify or dampen the initial control value in response to a perturbation in radiative heating. The amount by which these feedbacks modify the control value is typically proportional to the "output" or change in temperature, represented as δT:

$$\delta T = \delta T_0 + f \delta T \tag{28}$$

where "feedback factor" f controls the amplification

α_i – physical process

$$\delta T = \lambda \delta R_0 + \lambda \sum_i \frac{\partial R}{\partial \alpha_i} \frac{\partial \alpha_i}{\partial T} \partial T \tag{29}$$

To establish the equivalence between the previous result and equation (28), the feedback factor needs to be defined:

$$f = \lambda \sum_i \frac{\partial R}{\partial \alpha_i} \frac{\partial \alpha_i}{\partial T} \tag{30}$$

Solving equation (28) for δT [2]:

$$\delta T = \frac{\delta T_0}{1 - f} \tag{31}$$

The delayed oscillator model is a prominent theoretical model used to study the El Niño-Southern Oscillation (ENSO). In this model, the equation for the sea surface temperature anomaly in the eastern Pacific, denoted as T, is as follows:

$$\frac{dT}{dt} = bT(t) - cT(t - \tau) \tag{32}$$

b, c - positive constants
τ – time delay
Valuable insights into the nature of synoptic-scale motions in the tropics can be obtained through scale analysis methods, despite uncertainties surrounding the interaction between convective and synoptic scales. To facilitate the scale analysis, expressing the governing equations in the log-pressure coordinate system proves to be a convenient approach. This transformation simplifies the representation of atmospheric dynamics, making it easier to study the relationships and processes involved in the tropics' synoptic-scale motions and their interaction with convective phenomena [2].

$$\left(\frac{\partial}{\partial_t} + V \cdot \nabla + w^* \frac{\partial}{\partial z^*}\right) V + fk \times V = -\nabla \Phi \tag{33}$$

$$\partial \Phi / \partial z^* = RT/H \tag{34}$$

$$\partial u/\partial x + \partial v/\partial y + \partial w^*/\partial z^* - w^*/H = 0 \tag{35}$$

$$\left(\frac{\partial}{\partial t} + V \cdot \nabla\right) T + w^* N^2 H/R = \frac{J}{c_p} \tag{36}$$

$$\partial u/\partial x + \partial v/\partial y \leq U/L \tag{37}$$

However, when considering motions with vertical scales that are on par with the density scale height H, the analysis becomes more intricate [2]:

$$\partial w^*/\partial z^* - w^*/H \sim W/H \tag{38}$$

to ensure the balance between the horizontal divergence and vertical stretching terms in the continuity equation, the vertical velocity scale, denoted as W, must satisfy the constraint $W \leq HU/L$. This constraint establishes the relationship between the vertical velocity scale, the horizontal velocity scale U, and the characteristic length scale L [2].
As a next step, let's outline the characteristic scales for the various field variables in the following table.

Table 1. Scales characteristic

$H \sim 10^4$ m	vertical length scale
$L \sim 10^6$ m	horizontal length scale
$U \sim 10\,\mathrm{m\,s^{-1}}$	horizontal velocity scale
$W \leq HU/L$	vertical velocity scale
$\delta\Phi$	geopotential fluctuation scale
$L/U \sim 10^5$ s	timescale for advection

The comparison of the magnitude of the horizontal inertial acceleration with other terms helps determine the dominant forces influencing atmospheric motion at different scales [2]:

$$(V \cdot \nabla)V \sim U^2/L \tag{39}$$

$$|\partial V/\partial t|/|(V \cdot \nabla)\mathrm{V}| \sim 1 \tag{40}$$

$$|w^* \partial V/\partial z^*|/|(V \cdot \nabla)\mathrm{V}| \sim WL/UH \leq 1 \tag{41}$$

$$|fk \times V|/|(V \cdot \nabla)\mathrm{V}| \sim fL/U = R_0^{-1} \leq 1 \tag{42}$$

$$|\nabla\Phi|/|(V\cdot\nabla)\mathrm{V}|\sim\delta\Phi/U^2 \tag{43}$$

In situations where there is no precipitation, the primary mechanism driving diabatic heating is the emission of longwave radiation, which leads to a cooling effect on the troposphere at a rate of approximately $J/c_p \sim 1Kd^{-1}$. Given the small magnitude of actual temperature fluctuations, this radiative cooling is approximately offset by adiabatic warming resulting from subsidence [2].

$$w^*(N^2H/R)=J/c_p \tag{44}$$

J - represents the radiative flux,

c_p - the specific heat capacity at constant pressure.

For the tropical troposphere [2]:

$$N^2K/R\sim 3Kkm^{-1} \tag{45}$$

Vertical motion scale must satisfy [2]:

$$W\sim 0.3\ cm\ s^{-1} \tag{46}$$

$$WL/UH\sim 0.03 \tag{47}$$

3. APPLICABLE THEORY, NUMERICAL SIMULATIONS AND CONCLUSIONS

The temperature distribution in the mid-atmosphere is determined by radiation for the northern winter solstice from a radiation pattern that is run an annual cycle.

In reality, tropospheric temperatures, as well as cloudiness, are used to determine the upward radiative flux from the tropopause.

Vertical wind shear in the free atmosphere is generally lower than in the boundary layer, except in the vicinity of jet streams.

Given the aircraft speeds high flight at that altitude, the lift force variation is not a hazard, as is in the case of windshear lower level, but the turbulence produced in regions with windshear determines the phenomenon of clear-air turbulence for the prediction of which, the association with various diagnostic indices with windshear represents a solution currently used in Aeronautical Meteorology [3-10].

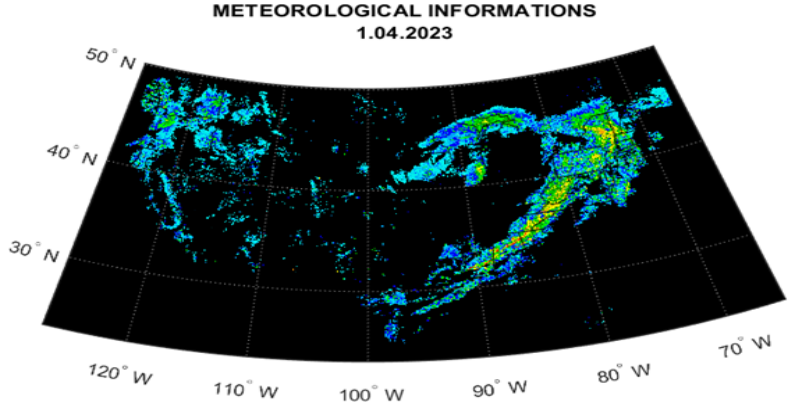

Fig. 1 Analysis Meteorological for Aircraft transmitted from Weather Support Center # 1.04.2023

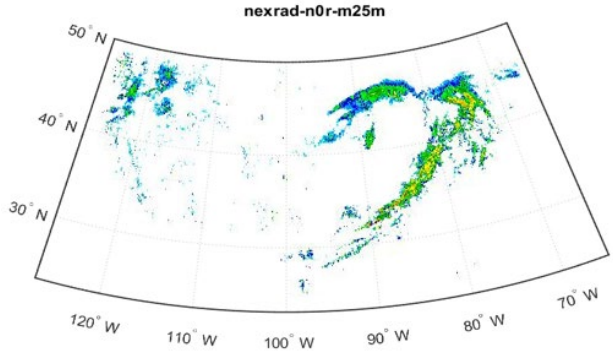

Fig. 2 Weather Units Aviation # 1.04.2023

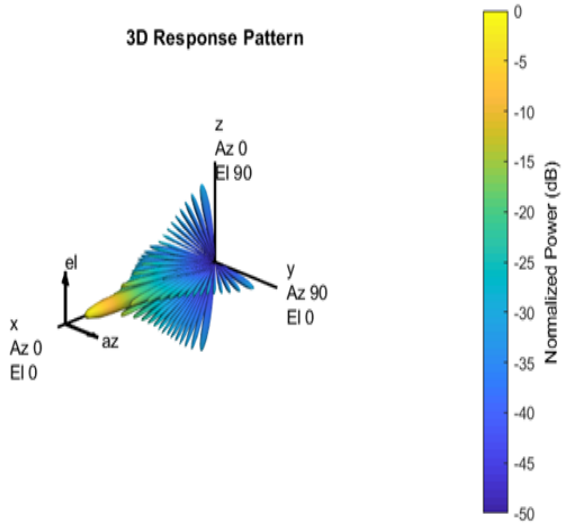

Fig. 3 D Pattern #Case Study 1

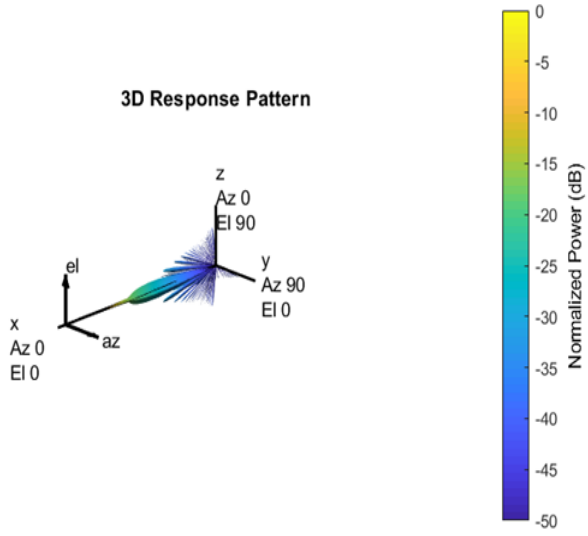

Fig. 4 D Pattern #Case Study 2

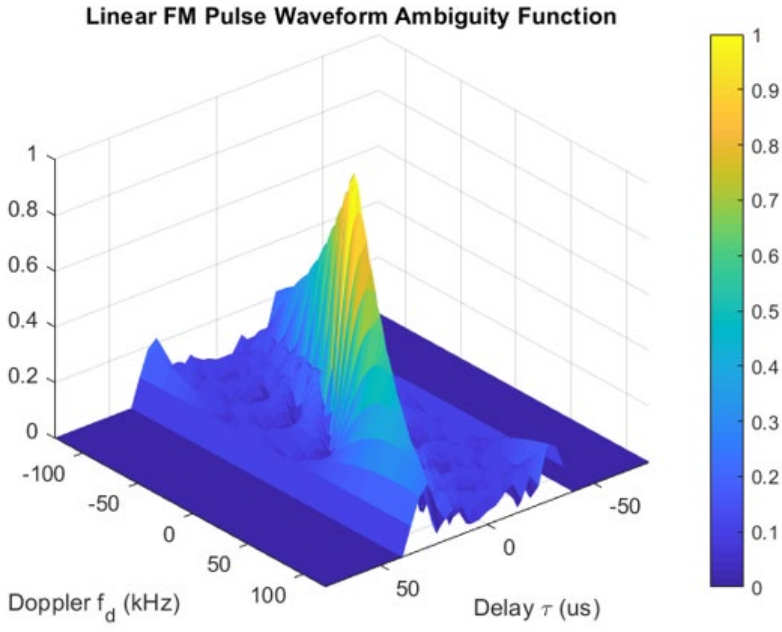

Fig. 5 Global Analysis Meteorological for Aircrafts Airport Weather Information # 1.04.2023

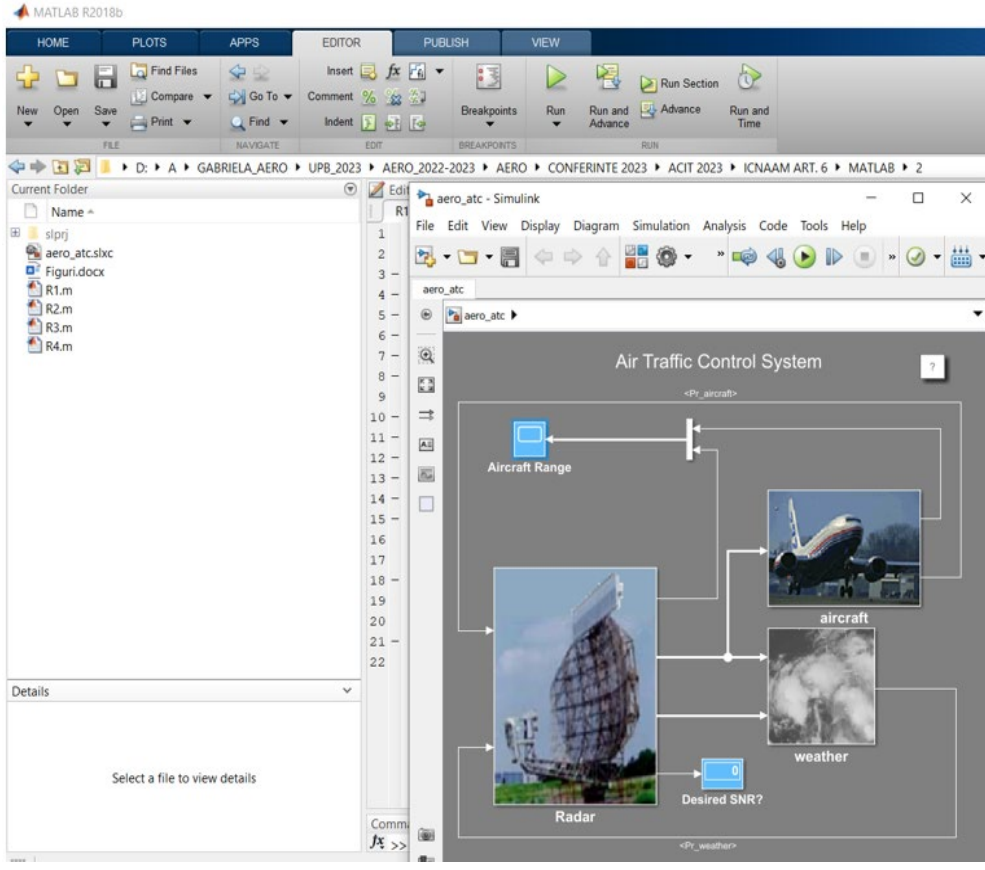

Fig. 6 Visualized meteorological information by Radar Display # Phase 1

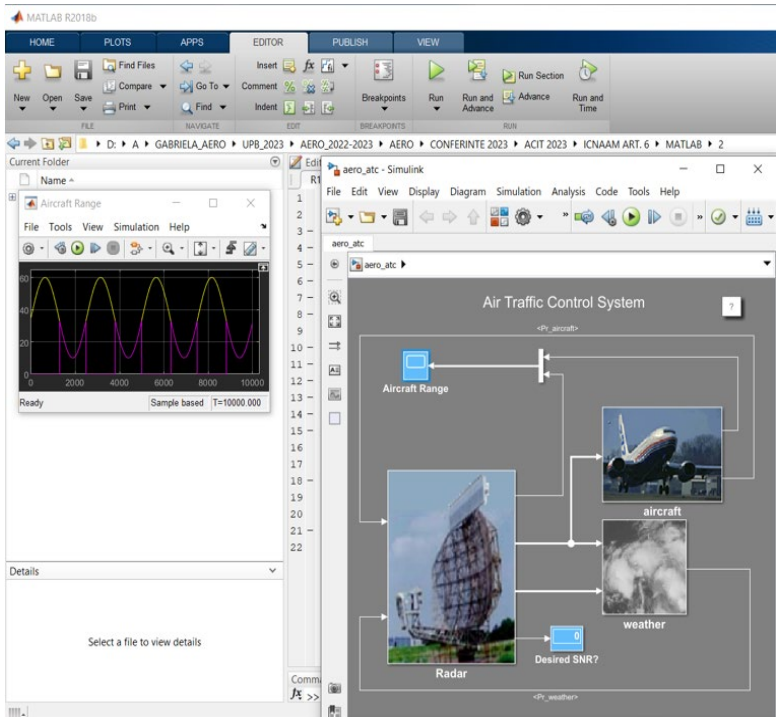

Fig. 7 Visualized meteorological information by Radar Display # Phase 2

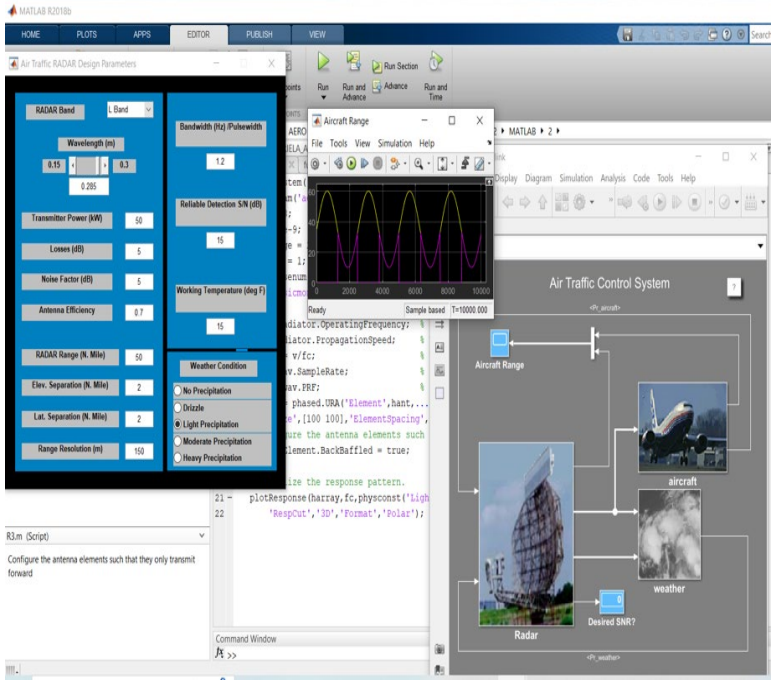

Fig. 8 Visualized meteorological information by Radar Display # Phase 3

This paper studies the vital importance of the meteorological information received by the pilot, regarding the intensity of the wind, but also its direction, which is included in the multitude of meteorological reports that are used before the flight of the aircraft, being necessary to know

the weather conditions in the runway area for the processes of landing and takeoff. The positions of the sensors for detecting the types of wind acting along the runways must be indicated in the meteorological reports, on those sections of the runway where the wind intensity data are representative. When wind direction and intensity data are available on multiple runways in use, the relevant route indications should also be presented with the wind data included in routine weather reports.

ACKNOWLEDGMENT

This work has been funded by the European Social Fund from the Sectorial Operational Programme Human Capital 2014-2020, through the Financial Agreement with the Title "Training of Ph.D. students and postdoctoral researchers in order to acquire applied research skills - SMART", Contract no. 13530/16.06.2022 - SMIS code: 153734.

REFERENCES

[1] * * * ATPL – Meteorology, CAE Oxford, 2020.
[2] J. R. Holton and G. J. Hakim, *An Introduction to Dynamic Meteorology*, Fifth Edition, 2013.
[3] D. McLean, *Automatic Flight Control System*, Prentice Hall International, 66 Wood Lane End, Hemel Hempstead, Herts HP2 4RG, 1990.
[4] B. L. Stevens and F. L. Lewis, *Aircraft Control and Simulation*, John Wiley, USA, 1992.
[5] * * * MATLAB Tutorials, 2022.
[6] * * * http://www.MathWorks, Inc. Aerospace Blockset, 2022.
[7] M. Rauw, *FDC 1.2.-A SIMULINK Toolbox for Flight Dynamics and Control Analysis*, May 10, 2001.
[8] B. Etkin, *Dynamics of Flight-Stability and Control*, Wiley, New York, John Wiley & Sons, Inc, London Chapman & Hall, Ltd, 3ND EDITIOn.
[9] L. Moysis, M. Tsiaousis, N. Charalampidis, M. Eliadou and I. Kafetzis, *An introduction to Control Theory Applications with Matlab*, August 31, 2015..
[10] D. Sheu, and Chuan-Tau Lan, Estimation of Turbulent Vertical Velocity from Nonlinear Simulations of Aircraft Response, *Journal of Aircraft*, Vol. **48**, No. 2, March-April, 2011, https://doi.org/10.2514/1.C031190.